



Evaluating the Hydraulic Conductivity of Modified Loess: A Machine Learning Approach

Guoliang Ran *, Tingting Li, Xi Zhang

School of Safety Engineering, Lanzhou Resources & Environment Voc-Tech University, Lanzhou, Gansu, 730000, China

*Ranguoliang@foxmail.com

Abstract. This study focuses on Lanzhou loess, exploring its permeability under various modification methods through falling-head permeability tests. The research identifies the impact of dry density, particle size characteristics, particle gradation, and additives on the permeability of modified loess. The impact of each influencing factor was assessed through grey relational analysis. Based on the experimental results and grey relational analysis, a predictive model was developed using the machine learning method of Support Vector Machines to estimate the hydraulic conductivity of modified loess Considering the combined effects of various factors. The results contribute to understanding the factors that affect the permeability of modified loess and provide a tool for more accurate predictions in engineering applications. The SVR model outperformed traditional multiple predictive models in terms of prediction accuracy, with lower root mean square errors and higher correlation coefficients. This study provides valuable insights into the modification of loess for engineering applications, offering a predictive tool for permeability in future infrastructure projects in loess-rich regions.

Keywords: Loess, hydraulic conductivity, dry density, additives, SVR model, Gray relational analysis

1 Introduction

The loess region, as a critical strategic area for advancing the "Western Development" and "Belt and Road" initiatives in the new era, supports the implementation of numerous major engineering projects while facing dual challenges of environmental protection and sustainable development. Given the stringent engineering requirements for loess in terms of foundation strength, settlement control, water stability, and durability, improving the engineering properties of loess has become an urgent and significant task [1].

Permeability as one of the key engineering properties of loess, is closely related to its deformation behavior and strength characteristics, profoundly influencing construction quality and long-term stability in practical projects [2]. However, the existing study on modified loess mostly focuses on mitigation of its collapsibility, with limited explora-

tion of its permeability. As a core parameter reflecting the water transmission and conduction capabilities of soil, the hydraulic conductivity is fundamental in hydrogeological analysis. Various factors, including initial moisture content [3], density [2], void ratio [4], compaction degree [5], external pressure [6], and temperature [7], significantly influence the hydraulic conductivity. Therefore, investigating the impacts of these factors on the variation law of hydraulic conductivity of loess is crucial for guiding soil improvement to meet engineering requirements. Loess as a porous medium, exhibits pronounced water sensitivity, with its mechanical properties deteriorating rapidly upon wetting or increased moisture content, resulting in significant strength reduction and accelerated deformation [8]. To eliminate collapsibility and improve mechanical properties of loess, engineering practices often employ dynamic compaction method, mechanical rolling method and chemical modification methods through chemical reactions induced by the addition of cement and other binding materials [9]. Current loess improvement techniques primarily rely on compaction and additive use, with relatively few studies focusing on adjusting particle size distribution and grading using excavated materials on-site. Additionally, research on the permeability variation patterns and prediction methods for Modified loess often centers on single influencing factors [10-14]. However, there is a lack of studies addressing the hydraulic conductivity variations under the joint influence of various factors, examine the extent of the influence of each variable, and developing predictive models for hydraulic conductivity considering multiple factors.

In this study, Malan loess was selected as the research object. A systematic investigation of the relationships between influencing factors and hydraulic conductivity was conducted through laboratory permeability tests. The extent of the influence of each variable was evaluated using the Grey Relational Analysis method. Furthermore, a saturated hydraulic conductivity prediction model for artificially modified materials was developed using the Support Vector Machine regression(SVR) algorithm. This study enriches the research findings on assessing the hydraulic conductivity of modified loess materials. The findings offer significant guidance for engineering construction in loess regions, particularly in the development and application of impervious materials for artificial water bodies.

2 Experimental Materials and Procedures

The materials employed in this research were obtained from Gaolan County, Gansu Province, China. The basic physical properties of the soil were obtained through laboratory testing (see Table 1). The laboratory soil tests followed the "Standard Test Methods for Geotechnical Testing" (GB50123-2019) [15]. Prior to testing, the field-collected soil samples were crushed to ensure that the particle size did not exceed 5 mm. Two methods were employed for soil improvement in this study:

- (1) The collected loess-type silt, loess (Q3), loess (Q2), clay-rich sandstone, and sandstone were mixed in varying proportions, followed by sample preparation and compaction. This process yielded different grain size characteristics, grain size distribution, and dry densities.

(2) Based on the modified soil samples from the first method, two types of additives were selected for further modification. The additives used in the experiment were lime and cement. The slaked lime (calcium hydroxide (CH), $\text{Ca}(\text{OH})_2$) of analytical grade was utilized, and the cement was Ordinary Portland Cement (OPC) with a grade of P. O42.5.

Finally, the hydraulic conductivity of the samples which were modified through the methods above was tested using the falling-head permeability experiment to evaluate the effect of the modifications. The sample preparation and testing procedures are shown in Figure 1, while the experimental plan and test results are presented in Table 2.

Table 1. Basic physical properties.

Name	Static Gravity Gs	Natural water content w (%)	Natural density $\rho(\text{g}/\text{cm}^3)$
Loess-type silt	2.75	9.7	1.49
Loess (Q3)	2.73	6.9	1.52
Loess(Q2)	2.46	11.9	1.80
Clay-rich sandstone	/	7.8	2.09



Fig. 1. Preparation and testing process.

Table 2. Experimental plan and results.

Sample number	Content of additives (%)	Additives type	d_{10} (mm)	d_{50} (mm)	d_{60} (mm)	C_u	C_c	ρ_d ($\text{g}\cdot\text{cm}^{-3}$)	k ($\text{cm}\cdot\text{s}^{-1}$)
SN1	0	/	0.0807	0.30	0.43	5.31	0.71	1.86	7.97×10^{-7}
SN2	0	/	0.0987	0.44	0.62	6.33	0.80	1.85	6.16×10^{-8}
SN3	0	/	0.1032	0.44	0.61	5.89	0.89	1.85	4.72×10^{-7}
SN4	0	/	0.0828	0.36	0.54	6.57	0.66	1.84	1.09×10^{-7}
SN5	0	/	0.0848	0.42	0.65	7.68	0.65	1.82	4.85×10^{-7}
SN6	0	/	0.0848	0.49	0.78	9.20	0.65	1.82	7.12×10^{-7}

SN7	0	/	0.0848	0.49	0.78	9.20	0.65	1.90	1.04×10^{-7}
SN8	0	/	0.0848	0.49	0.78	9.20	0.65	1.82	7.12×10^{-7}
SN9	0	/	0.0848	0.49	0.78	9.20	0.65	1.77	5.12×10^{-6}
SN10	0	/	0.0848	0.49	0.78	9.20	0.65	1.69	9.12×10^{-6}
SN11	9	OPC	0.091	0.50	0.76	8.30	0.65	1.62	2.14×10^{-6}
SN12	12	OPC	0.090	0.50	0.75	8.31	0.65	1.63	7.10×10^{-7}
SN13	15	OPC	0.090	0.50	0.75	8.31	0.65	1.62	2.80×10^{-7}
SN14	9	OPC	0.090	0.42	0.65	7.02	0.64	1.63	2.03×10^{-7}
SN15	12	OPC	0.090	0.42	0.65	7.02	0.64	1.62	3.86×10^{-6}
SN16	15	OPC	0.090	0.42	0.65	7.02	0.64	1.65	1.80×10^{-7}
SN17	6	CH	0.084	0.50	0.79	9.19	0.65	1.78	8.02×10^{-7}
SN18	9	CH	0.084	0.50	0.79	9.19	0.65	1.80	6.89×10^{-7}
SN19	12	CH	0.084	0.50	0.79	9.19	0.65	1.80	6.20×10^{-7}
SN20	5	OPC	0.084	0.50	0.79	9.19	0.65	1.80	3.60×10^{-7}
SN21	9	OPC	0.084	0.50	0.79	9.19	0.65	1.81	2.61×10^{-7}
SN22	9	OPC	0.084	0.50	0.79	9.19	0.65	1.48	6.31×10^{-8}
SN23	12	OPC	0.084	0.50	0.79	9.19	0.65	1.63	7.10×10^{-7}
SN24	15	OPC	0.084	0.50	0.79	9.19	0.65	1.62	5.22×10^{-6}
SN25	5	OPC	0.084	0.50	0.55	6.58	0.65	1.80	3.71×10^{-7}
SN26	5	OPC	0.084	0.50	0.66	7.69	0.65	1.82	3.65×10^{-7}
SN27	15	OPC	0.084	0.50	0.79	9.19	0.65	1.64	8.48×10^{-7}
SN28	15	OPC	0.084	0.50	0.79	9.19	0.65	1.75	5.01×10^{-7}
SN29	15	OPC	0.084	0.50	0.79	9.19	0.65	1.81	7.61×10^{-8}

1. Particle size parameters (d_{10} , d_{50} , d_{60}) define gradation characteristics, where d_x denotes the particle diameter for which $x\%$ of the soil mass is finer.

2. C_u (d_{60}/d_{10}) quantifies gradation uniformity; C_c [$(d_{30})^2/(d_{10} \cdot d_{60})$] evaluates gradation curve shape.

3. Hydraulic conductivity (k) represents saturated soil permeability under laminar flow conditions.

3 Experimental Results and Interpretation

3.1 Single-Variable Analysis and Results of Modified Loess

3.1.1 Effect of Additives on Hydraulic Conductivity.

In the two test groups, SN11, SN12, SN13 and SN14, SN15, SN16, the grain size characteristics, grain size distribution and dry density remained consistent, while the cement additive content varied. The results of these tests are shown in Figure 2. It can be observed that the hydraulic conductivity decreased with the increasing cement content.

In the SN11, SN12, and SN13 group, as the cement content raised from 9% to 12%, the hydraulic conductivity decreased by a factor of 3.01. As the cement content further increased from 12% to 15%, the hydraulic conductivity decreased by a factor of 2.53,

indicating a diminishing rate of reduction in the hydraulic conductivity with higher cement content.

When cement is used as an additive to improve loess, the reduction in hydraulic conductivity tends to reach a limit within the typical range of cement content for engineering applications. Based on the conditions of this study, within the cement content range of 9% to 15%, this limit was determined to be approximately $7.61 \times 10^{-8} \text{ cm/s}$ (SN29). In comparison, for a sample with the same dry density but without cement (SN8), the hydraulic conductivity was $7.12 \times 10^{-7} \text{ cm/s}$, which is 9.36 times higher than that of the cement-modified sample.

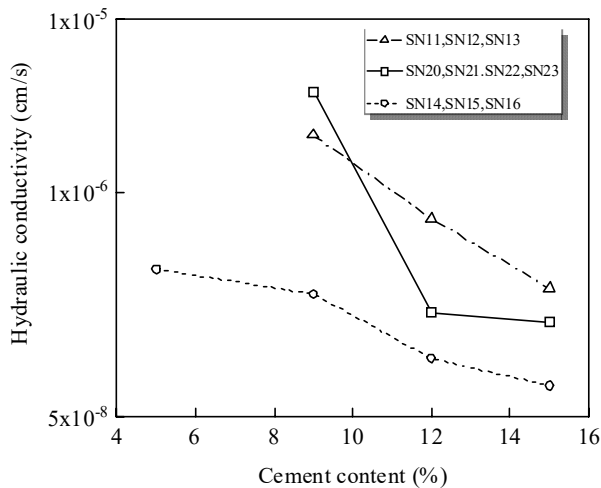


Fig. 2. Correlation between cement content and hydraulic conductivity.

During the tests, the low clay particle content in the tested soil resulted in incomplete filling of all voids between fine particles during the initial formation of cement hydration products. Consequently, the hydraulic conductivity of the modified loess with cement decreased rapidly with cement content increasing. However, when the cement content reached a level sufficient to fill most of the voids between fine particles, further increases in cement content had a diminishing effect on reducing the hydraulic conductivity.

This phenomenon is evident in Figure 2, where the rate of decrease in hydraulic conductivity significantly slows once the cement content exceeds 12%. This implies that the pore structure plays a significant role in determining the hydraulic conductivity of modified loess. Thus, under the same additive ratio, minimizing the void ratio and enhancing the dry density of cement-modified loess can more effectively lower its hydraulic conductivity.

3.1.2 Effect of Dry Density on Hydraulic Conductivity.

Figure 3 illustrates samples' hydraulic conductivity under varying dry densities. The two sets of tests are SN7, SN8, SN9, SN10, and SN24, SN27, SN28, SN29, respec-

tively. The former does not include any additives, while the latter incorporates 15% cement. For each group of samples, the grain size characteristics and grain size distribution remained constant, with dry density being the only variable. There was an inverse relationship between hydraulic conductivity and dry density, decreasing as the dry density increased. Both curves demonstrated a distinct turning point. For the first group (SN7, SN8, SN9, SN10), the turning point occurred at $\rho_d=1.65 \text{ g}\cdot\text{cm}^{-3}$, while for the second group (SN24, SN25, SN28, SN29), it was observed at $\rho_d=1.82 \text{ g}\cdot\text{cm}^{-3}$. Beyond the turning point, further increases in dry density resulted in only marginal reductions in the hydraulic conductivity.

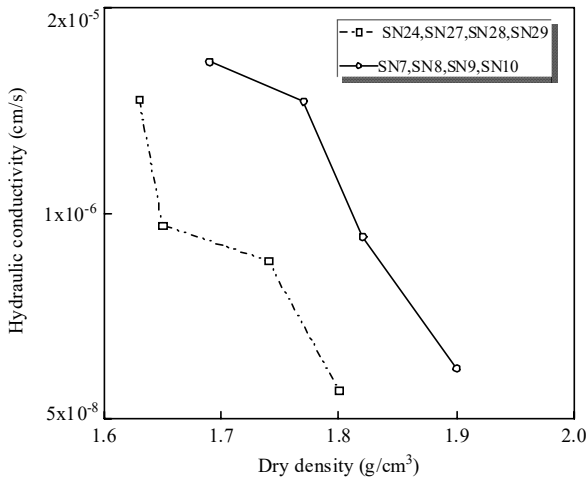


Fig. 3. Correlation between dry density and hydraulic conductivity.

Compared to unimproved samples, cement-modified loess exhibited significantly lower hydraulic conductivity under similar dry density conditions. This reduction is attributed to the hydration reaction of cement within the modified loess. The hydration process lead to the gradual formation of hydration products on the surfaces of soil particles and within the voids, effectively filling larger pores. Additionally, the hydration reaction significantly reduces the content of free water, thereby increasing density and further reducing the hydraulic conductivity.

However, the higher the cement content, the lower the dry density that the modified loess can achieve under the same compaction effort. This is primarily due to the fine particle size of cement, which makes it difficult to achieve effective mixing with the soil and limits the achievable compaction density.

3.1.3 Effect of Particle Size Characteristics on the Hydraulic conductivity.

In the group of tests SN1, SN2, SN3, SN4, SN5, and SN6, with no additives were included, and the dry density of the samples was controlled within the narrow range. The average value is $1.85 \text{ g}\cdot\text{cm}^{-3}$, and the standard deviation accounts for less than 0.75% of the mean. Given the minimal fluctuation in dry density, it can be assumed that

the hydraulic conductivity of these samples was not significantly affected by dry density.

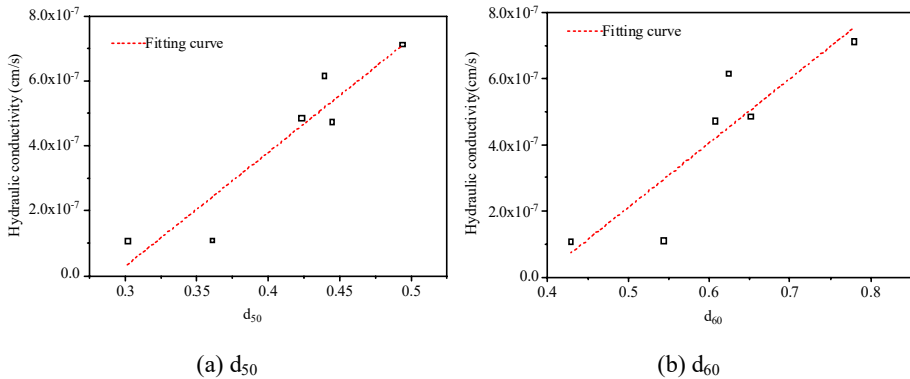


Fig. 4. Relationship curve between grain size characteristics and hydraulic conductivity.

Unlike findings from studies on sandy soils, the effective particle size d_{10} of modified loess does not exhibit a strong correlation with the hydraulic conductivity. This difference arises from the structural dissimilarities between loess and sandy soils.

The mean particle size d_{50} is a crucial parameter for assessing soil grain size distribution, as it reflects the overall size of soil particles. When the void ratio and grain size characteristics remain constant, the total pore volume of the soil stabilizes. As the mean particle size d_{50} increases, the mean pore size of the soil also grows. This study altered the mean particle size of samples by mixing different types of soils to explore its relationship with the hydraulic conductivity.

As shown in Figure 4, the hydraulic conductivity exhibits an approximately linear positive correlation with the mean particle size d_{50} , with goodness of fit is 0.8561. An increase in the mean grain size causes larger interparticle pore diameters, which in turn leads to a greater cross-sectional area of the voids. Consequently, the head loss through the pores decreases, and the water flow velocity increases. According to Darcy's law, the hydraulic conductivity increases. Moreover, as depicted in Figure 4, the hydraulic conductivity also shows an approximately linear positive correlation with the limiting particle size d_{60} , with goodness of fit is 0.7915. As the limiting grain size d_{60} increases, the variation in the hydraulic conductivity becomes more pronounced, with the maximum difference reaching 6.65 times.

3.1.4 Effect of Particle Size Distribution on Hydraulic Conductivity.

There was no significant correlation observed between the hydraulic conductivity and both the uniformity coefficient and curvature coefficient. However, the product of these two coefficients can be fitted using a linear function, with a goodness of fit of 0.8464, as shown in the in Figure 5.

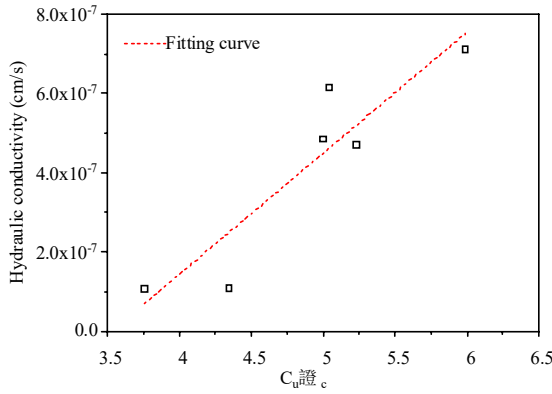


Fig. 5. $C_u \times C_c$ versus hydraulic conductivity curve.

3.2 Grey Relational Analysis

The factors influencing the hydraulic conductivity are intricate, and the interaction mechanisms between these factors are complex and not yet well understood. As a result, it is difficult to construct an accurate predictive model through analytical methods or empirical formulas. In light of this, this study employs the grey relational analysis method to first clarify the extent to which each factor affects the hydraulic conductivity. Building on the results, a prediction model for hydraulic conductivity is developed using SVR, integrating multiple factors.

The hydraulic conductivity is set as the reference sequence, and d_{50} , d_{60} , d_{10} , dry density, C_u , C_c , type of additives, and additive content are set as the comparative sequences. The analysis results are shown in Figure 6.

From Figure 6, it can be seen that the factor with the greatest influence on the hydraulic conductivity of the modified loess is the type of additive, followed by C_c . This indicates that a reasonable grain size distribution and the use of additives can significantly reduce the hydraulic conductivity.

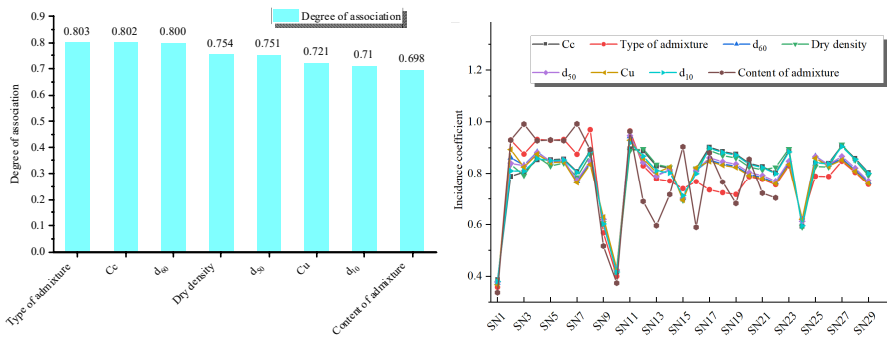


Fig. 6. Result of Gray Correlation Analysis.

3.3 Support Vector Machine (SVR) Model for Predicting the Hydraulic Conductivity

Based on the findings in the previous section, this section directly provided prediction model using SVR through experimental data. The analysis of the influence of multiple factors on the hydraulic conductivity is transformed into the identification of regression model parameters.

Support Vector Regression (SVR) analysis can be implemented using MATLAB's built-in toolbox, Based on prior research findings[16-18], radial basis function (RBF)-type kernel functions demonstrate superior suitability for regression tasks. In this study, an RBF kernel was consequently adopted for the SVR regression framework. Prior to model training, parameter optimization was performed to identify the optimal penalty coefficient C and kernel parameter gamma. The parameter C , which governs the trade-off between model complexity (margin width) and empirical error tolerance, critically influences generalization performance. A higher ' value indicates lower tolerance for errors, increasing the risk of overfitting, whereas excessively small C values may lead to underfitting, both scenarios degrading generalization-capability. The parameter gamma, intrinsic to the RBF kernel, implicitly determines the feature space distribution by controlling the influence radius of individual training samples. Higher gamma values result in fewer support vectors, reducing computational complexity during training and inference, while smaller gamma values promote denser support vector distributions.

Through systematic parameter tuning, the optimal parameters for this study were determined as $C=1$ and $\gamma=8$, achieving a balance between model accuracy computational efficiency.

Comparison prediction experiments were conducted on the dataset in Table 1 using multiple linear regression, Back Propagation Neural Network, and SVR. The fitting results are detailed in Table 3 and Figure 7, demonstrating that the model shows high accuracy in predicting the hydraulic conductivity of modified loess. The regression results and their error analysis are shown in Figures 7 and 8, respectively.

A Taylor diagram is used to analyze the deviation between the Analytical solutions of the three models and the Laboratory readings. The analysis results are shown in Figure 8. The results indicate that the SVR prediction model has the closest predicted values to the actual values, with the strongest correlation and the smallest root mean square error, showing the highest prediction accuracy. The multi-linear regression model, on the other hand, exhibited the lowest prediction accuracy and the highest error.

Table 3. Predicted and observed values from the SVR model.

Sample number	Laboratory readings	Analytical solutions
SN26	3.65×10^{-7}	4.17×10^{-7}
SN27	8.48×10^{-7}	8.08×10^{-7}
SN28	5.01×10^{-7}	5.74×10^{-7}
SN29	7.61×10^{-7}	9.20×10^{-7}

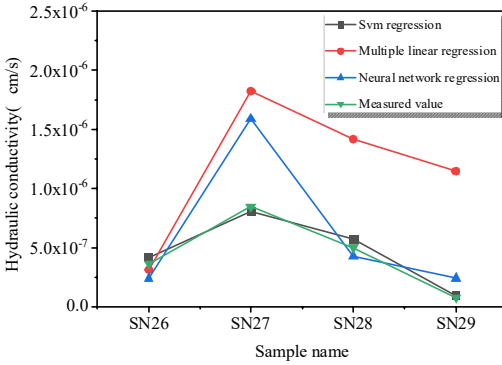


Fig. 7. Comparison between predicted and observed values.

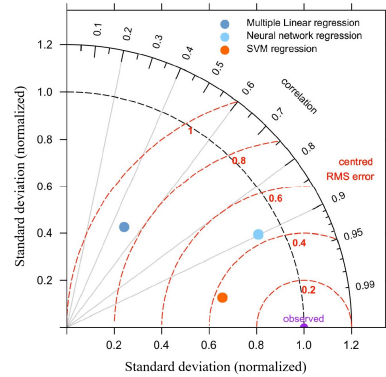


Fig. 8. Error analysis by Taylor diagrams

4 Conclusion

(1) As the dry density increases, the hydraulic conductivity of modified loess decreases. This decreasing trend exhibits a clear inflection point. Once the dry density exceeds this inflection point, further increases in dry density result in a relatively smaller decrease in hydraulic conductivity.

(2) With consistent particle characteristics, gradation, and dry density, the hydraulic conductivity of modified loess decreases as the content of additives (such as cement and lime) increases. Notably, when the particle size is larger and the C_u value is smaller, the influence of cement content on the hydraulic conductivity is more significant.

(3) There exists a strong linear positive correlation between parameters such as the mean particle size, limiting particle size, the product of uniformity coefficient and curvature coefficient, and the hydraulic conductivity.

(4) The prediction results of the SVR model are notably superior to the other two models used in this study, demonstrating smaller prediction errors.

Acknowledgments

This work was supported Research Capability Enhancement Plan of Lanzhou Resources & Environment Voc-Tech University. (X2024A-19).

References

- Bai, J. G., Kou, W. Q., & Li, H. J. (2024). Numerical simulation of the deformation behavior of a composite foundation consisting of rubber particle loess-cfg under dynamic loading. *Journal of Vibrio engineering*, 26(5).
- Li, Z., Cui, Z., Wang, Y., et al. (2011). Experimental study on the engineering characteristics of improved soil. *Advanced Materials Research*, 1068, 1234-1240.

3. Liu, J. Y., Li, X., Xue, Q., & Guo, Z. Z. (2020). Experimental study on air permeability and microscopic mechanism of intact and remolded Malan loess, Loess Plateau, China. *Bulletin of Engineering Geology and the Environment*.
4. Xu, P., Zhang, Q., Qian, H., et al. (2021). An investigation into the relationship between saturated permeability and microstructure of remolded loess: A case study from Chinese Loess Plateau. *Geoderma*, 382, 114652.
5. Li, P., Pan, Z., Xiao, T., Wang, J. (2023). Effects of molding water content and compaction degree on the microstructure and permeability of compacted loess. *Acta Geotechnica*, 18(2), 921-936.
6. Li, X., Liu, J., Guo, Z., et al. (2018). Study on the relationship between pore structure parameters and permeability of Malan loess. *Journal of Engineering Geology*, 26(6), 1415-1423.
7. Zhao, Z., Wang, T., Jin, X., Zhang, L., Zhu, X., Ruan, J. (2023). A new model of temperature-dependent permeability coefficient and simulation of pipe leakage produced by immersion of loess foundation. *Bulletin of Engineering Geology and the Environment*, 82(1), 1-12.
8. Li, P., Vanapalli, S., Li, T. (2016). Review of collapse triggering mechanism of collapsible soils due to wetting. *Journal of Rock Mechanics and Geotechnical Engineering*, 8(2), 256-274.
9. Yuan, Y., Jiang, Y., Cai, L., Fan, J., Deng, C., Xue, J. (2021). Influencing factors and prediction model for the anti-erosion performance of cement-improved loess compacted using different compaction methods. *Advances in Materials Science and Engineering*, 2021, 1-13.
10. Zhang, S. Y., & Zhang, W. Y. (2025). Experimental study on freeze-thaw characteristics of loess improved by lignin-slag carbonization synergy. *Water Resources and Hydropower Technology (Chinese and English)*, 1-22.
11. Meng, M. Q., Wang, M. Z., Liu, Y. L., Zhang, Y. Y., Liu, G. Y., & Ru, H. (2025). Strength characteristics and microscopic mechanism of phosphogypsum-polypropylene fiber modified loess. *Journal of Civil and Environmental Engineering (Chinese and English)*, 1-11.
12. Zhou, G. X., Huang, Z. J., Chen, W., Wan, Y. G., Fan, X., Wang, Y. Y., ... & Zhao, E. S. (2024). Influence of delay time on mechanical properties of fly ash-modified loess and mechanism analysis. *Science Technology and Engineering*, 24(33), 14364-14370.
13. Liu, J. (2024). Experimental analysis of road performance improvement for collapsible loess using lignin modification. *Heilongjiang Journal of Transportation Science and Technology*, 47(11), 71-74.
14. Wang, Q., Wang, L. M., Liu, Z. Z., & et al. (2024). Engineering properties and reinforcement mechanisms of lignin-improved loess. *Chinese Journal of Geotechnical Engineering*, 46(S2), 150-154+215.
15. Standard Test Methods for Geotechnical Testing (GB50123-2019). China Planning Press, Beijing, China, 2019.
16. Akshaya, R., & Premalatha, K. (2024). Prediction of soil compression index using svm and knn. IOP Publishing Ltd.
17. Huang, Y. (2023). Improved svm-based soil-moisture-content prediction model for tea plantation. *Plants* (2223-7747), 12(12).
18. Lee, J. M., Ko, K. S., & Yoo, K. (2023). A machine learning-based approach to predict groundwater nitrate susceptibility using field measurements and hydrogeological variables in the nonsan stream watershed, south korea. *Applied Water Science*, 13(12).

Open Access This chapter is licensed under the terms of the Creative Commons Attribution-NonCommercial 4.0 International License (<http://creativecommons.org/licenses/by-nc/4.0/>), which permits any noncommercial use, sharing, adaptation, distribution and reproduction in any medium or format, as long as you give appropriate credit to the original author(s) and the source, provide a link to the Creative Commons license and indicate if changes were made.

The images or other third party material in this chapter are included in the chapter's Creative Commons license, unless indicated otherwise in a credit line to the material. If material is not included in the chapter's Creative Commons license and your intended use is not permitted by statutory regulation or exceeds the permitted use, you will need to obtain permission directly from the copyright holder.

